BJP BRITISH JOURNAL OF PHARMACOLOGY

BPS BRITISH PHARMACOLOGICAL SOCIETY

British Journal of Pharmacology (2010), 160, 260–269

0007-1188/10
www.brjpharmacol.org

RESEARCH PAPER

Novel ruthenium complexes as potential drugs for Chagas's disease: enzyme inhibition and *in vitro*/*in vivo* trypanocidal activity

Jean Jerley Nogueira Silva[1,2], Paulo Marcos Matta Guedes[3], Aderson Zottis[1], Tatiane Luciano Balliano[1], Francisco Ordelei Nascimento Silva[4], Luiz Gonzaga França Lopes[4], Javier Ellena[1], Glaucius Oliva[1], Adriano Defini Andricopulo[1], Douglas Wagner Franco[2] and João Santana Silva[3]

[1]*Departamento de Física e Informática, Instituto de Física de São Carlos, Universidade de São Paulo, São Carlos, SP, Brazil,* [2]*Departamento de Química e Física Molecular, Instituto de Química de São Carlos, Universidade de São Paulo (USP), São Carlos, SP, Brazil,* [3]*Departamento de Bioquímica e Imunologia, Faculdade de Medicina de Ribeirão Preto, Universidade de São Paulo, Ribeirão Preto, SP, Brazil and* [4]*Departamento de Química Orgânica e Inorgânica, Universidade Federal do Ceará, Fortaleza, CE, Brazil*

Background and purpose: The discovery of the pharmacological functions of nitric oxide has led to the development of NO donor compounds as therapeutic agents. A new generation of ruthenium NO donors, *cis*-[Ru(NO)(bpy)$_2$L]X$_n$, has been developed, and our aim was to show that these complexes are able to lyse *Trypanosoma cruzi in vitro* and *in vivo*.
Experimental approach: NO donors were incubated with *T. cruzi* and their anti-*T. cruzi* activities evaluated as the percentage of lysed parasites compared to the negative control. *In vivo*, trypanocidal activity was evaluated by observing the levels of parasitaemia, survival rate and elimination of amastigotes in mouse myocardial tissue. The inhibition of GAPDH was monitored by the biochemical reduction of NAD^+ to NADH.
Key results: The NO donors *cis*-[Ru(NO)(bpy)$_2$imN](PF$_6$)$_3$ and *cis*-[Ru(NO)(bpy)$_2$SO$_3$]PF$_6$, at a dose of 385 nmol·kg^{-1}, yielded survival rates of 80 and 60%, respectively, in infected mice, and eradicated any amastigotes from their myocardial tissue.
Conclusions and implications: The ruthenium compounds exhibited potent *in vitro* and *in vivo* trypanocidal activities at doses up to 1000-fold lower than the clinical dose for benznidazole. Furthermore, one mechanism of action of these compounds is via the *S*-nitrosylation of Cys166 of *T. cruzi* GAPDH. Thus, these compounds show huge potential as candidates for the development of new drugs for the treatment of Chagas's disease.
British Journal of Pharmacology (2010) **160,** 260–269; doi:10.1111/j.1476-5381.2009.00524.x; published online 26 January 2010
This article is commented on by Machado *et al.*, pp. 258–259 of this issue. To view this commentary visit http://dx.doi.org/10.1111/j.1476-5381.2010.00662.x and to view a related paper in this issue by Guedes *et al.* visit http://dx.doi.org/10.1111/j.1476-5381.2010.00576.x

Keywords: NO donors; *Trypanosoma cruzi*; medicinal inorganic chemistry; GAPDH; ruthenium

Abbreviations: ATC, acute toxic class method; BF_4^-, tetrafluoroborate ion; BT, trypomastigote forms of *Trypanosoma cruzi* in the bloodstream; Bz, benznidazole; 1,3-DPG, 1,3-bisphosphoglycerate; $E_{(NO^+/NO^0)}$, reduction potential of the $Ru^{II}NO^+/Ru^{II}NO^0$ couple; EF, epimastigote forms of *T. cruzi*; gGAPDH, *T. cruzi* glycosomal glyceraldehyde-3-phosphate dehydrogenase (EC 1.2.1.12; P22513); G-3-P, glyceraldehyde-3-phosphate; GV, gentian violet; IC_{50}^{epi}, concentration corresponding to 50% anti-proliferative activity on epimastigote forms after 72 h of incubation; IC_{50}^{GAPDH}, concentration corresponding to 50% inhibitory activity on *T. cruzi* GAPDH; IC_{50}^{try}, concentration corresponding to 50% trypanocidal activity on trypomastigote forms after 24 h of incubation; imN, imidazole; INF-γ, gamma interferon; k_{-NO}, specific rate constant for NO release; 1-miN, 1-methyl imidazole; NHE, normal hydrogen electrode; NO, nitric oxide; PBS, phosphate-buffered saline; PF_6^-, hexafluorophosphate ion; 3-PGA, 3-phosphoglycerate; PGK, phosphoglycerate kinase; SNP, sodium nitroprusside; SO_3^2, sulphite ion; TGF-β, transforming growth factor-β

Introduction

Neglected tropical diseases encompass a group of pathologies that disproportionately affect resource-constrained regions of the world (Sachs, 2007). In tropical and subtropical countries, the vicious cycle of poverty, disease and underdevelopment is widespread (Reddy *et al.*, 2007). The burden of disease resulting from neglected tropical diseases is very high, leading to millions of deaths worldwide (Reddy *et al.*, 2007). Chagas's disease, caused by the protozoan parasite *Trypanosoma cruzi*, is a major public health problem and one of the leading causes of morbidity, long-term disability and mortality from cardiovascular diseases in Latin America (Engels & Savioli, 2006). It is estimated that 13 million people are directly affected in Central and South America, with nearly another 75 million living in high-risk areas (WHO, 2005). In spite of the alarming health, economic and social consequences of this parasitic infection, no vaccines are available at present, and the limited existing drug therapy (e.g. benznidazole and nifurtimox) suffers from a series of drawbacks including poor efficacy and serious side effects (Castro *et al.*, 2006). Therefore, there is an urgent need for new, safe and effective drugs for human use. In this context, the identification of novel targets and the design of promising drug candidates are major challenges for the treatment of Chagas's disease.

The control of *T. cruzi* infection in vertebrate hosts is dependent on the activation of macrophages and NO production, which is involved in intracellular parasite destruction (Silva *et al.*, 2003). Thus, the pharmacological modulation of the host's immune response against *T. cruzi* through the control of the levels of NO has been gaining substantial interest as a potentially valuable chemotherapeutic target (Maya *et al.*, 2007). In a recent study, we showed that the ruthenium NO donors *trans*-$[Ru(NO)(NH_3)_4L]^{3+}$ L = *N*-heterocyclic, H_2O, SO_3^{2-} and $P(OEt)_3$ are able to lyse trypomastigotes of *T. cruzi* present in the bloodstream (BT), *in vitro* and *in vivo*, by an NO-dependent mechanism (Silva *et al.*, 2007; 2009). In contrast, the glycolytic pathway of trypanosomatids has also been extensively investigated as a promising biochemical target for small molecule intervention. The form of trypanosomatids present in the bloodstream has no functional tricarboxylic acid cycle and is highly dependent on glycolysis for ATP production (Souza *et al.*, 1998; Verline *et al.*, 2001). This vital dependence on glycolysis as a source of energy makes the glycolytic enzymes attractive targets for drug design. One of the key enzymes in the glycolytic cascade, glyceraldehyde-3-phosphate dehydrogenase (GAPDH; EC 1.2.1.12), possesses important structural differences when compared to the homologous protein from the mammalian host (about 45% sequence identity), and is thought to be an attractive target for the development of novel anti-trypanosomatid agents (Guido *et al.*, 2008).

In the present study, we synthesized a new class of ruthenium NO donors, *cis*-$[Ru(NO)(bpy)_2L]^{n+}$, *cis*-$[Ru(H_2O)(bpy)_2L]^{n+}$ and *cis*-$[Ru(NO_2)(bpy)_2L]^{n+}$ where L = imidazole (imN), 1-methylimidazole (1-miN) or sulphite ion (SO_3^{2-}), and evaluated their effects in cell cultures and animal models, as well as in enzyme kinetic and crystallization assays.

Correspondence: J. J. N. Silva, Av. Trabalhador São-Carlense, 400 CP 780 São Carlos, SP; CEP 13566-970, Brazil. E-mail: jjerley@usp.br
Received 22 May 2009; revised 22 May 2009, 22 August 2009; accepted 26 August 2009

Methods

Synthesis of the ruthenium compounds

The ruthenium complexes *trans*-$[Ru(NO)(NH_3)_4imN](BF_4)_3$ (Borges *et al.*, 1998), and *cis*-$[Ru(NO)(bpy)_2imN](PF_6)_3$, *cis*-$[Ru(NO)(bpy)_2$1-miN$](PF_6)_3$, *cis*-$[Ru(NO)(bpy)_2SO_3]PF_6$, *cis*-$[Ru(bpy)_2(H_2O)SO_3]$, *cis*-$Na[Ru(bpy)_2(NO_2)SO_3]$, *cis*-$[Ru(bpy)_2imN(NO_2)]PF_6$ and *cis*-$[Ru(bpy)_2(H_2O)imN](PF_6)_2$ (Da Silva *et al.*, 2006) were synthesized and characterized as described previously.

Single-crystal X-ray diffraction experiment

The crystallization assays were performed by the slow evaporation method from acetone under a saturating condition at 298K. After 2 days, a suitable red single crystal was obtained. Intensity data were collected at room temperature (293K) with graphite monochromated MoKα radiation (λ = 0.71073 Å), using an Enraf-Nonius Kappa-CCD diffractometer. The unit cell was refined using the software Collect (Enraf-Nonius, 1997) and Scalepack (Otwinowski *et al.*, 1997), and the final cell parameters were obtained on all reflections. Data were collected up to 26.41° in θ, giving 15 234 Bragg reflections. Data reduction was carried out using the software Denzo-SMN and Scalepack, and the program XdisplayF was used for visual representation of the data. No significant absorption coefficient (0.828 mm^{-1}) was observed. Thus, a semi-empirical absorption correction based on equivalents was applied (Blessing, 1995). The structure was solved using the software SHELXS-97 (Sheldrick, 1997), and refined using the software SHELXL-97, where the C, N and O atoms were clearly solved, and full-matrix least square refinement of these atoms with anisotropic thermal parameters was carried out. The hydrogen atoms were positioned stereochemically and were refined with the riding model. The details concerning the data collection and structure refinement were prepared using WinGX (version 1.70.01) (Farrugia, 1999). The ORTEP-3 (Farrugia, 1997) program was used to prepare the figures. The complete crystallographic data were deposited at the Cambridge Crystallographic Data Centre as supplementary publication no. CCDC 702919. Copies of the data are available on application to The Director, CCDC, 12 Union Road, Cambridge CB2 1EZ, UK (e-mail: deposit@ccdc.cam.ac.uk or http://www.ccdc.cam.ac.uk).

Enzymatic inhibition studies

All enzymatic assays were carried out in triplicate at 25°C, as previously described (Pereira *et al.*, 2008). The reaction mixture contained 100 mM triethanolamine, HCl buffer (pH 7.5), 1 mM EDTA, 1 mM 2-mercaptoethanol, 30 mM $NaHAsO_4$ $7H_2O$, 400 μM NAD^+, 20 nM GAPDH and 300 μM D-glyceraldehyde-3-phosphate. The biochemical reduction of NAD^+ to NADH was monitored at 340 nm for 8 min using a Cary 100 Bio UV/Vis equipped with a Peltier-thermostatted

multicell changer and a temperature controller. Values of IC_{50}^{GAPDH} (concentration corresponding to 50% inhibitory activity on *T. cruzi* GAPDH) were independently determined by making rate measurements for at least five inhibitor concentrations. The values represent means of at least three individual experiments, and were estimated from the collected data employing the SigmaPlot enzyme kinetics module.

Animals, parasites and experimental infection

Balb/c female mice, 6–8 weeks old, were cared for according to institutional ethical guidelines, and all procedures and experimental protocols were approved by the Ethics Committee in Animal Research of the FMRP-USP. The *T. cruzi* Y strain was used in all experiments (Silva and Nussenzweig, 1953). Trypomastigote forms were purified from a fibroblast cell line (LLC-MK_2) and routinely passed in mouse, whereas epimastigote forms were grown in LIT medium (Silva *et al.*, 2008).

Evaluation of the trypanocidal activity in vitro

Trypanosoma cruzi bloodstream trypomastigotes (BT) and epimastigotes were re-suspended at 1.0×10^6 parasites·mL^{-1} in either non-infected blood samples or in LIT medium containing 10% fetal bovine serum (FBS), respectively (Silva *et al.*, 2007; 2008). Triplicate samples were treated with the test compounds diluted in phosphate-buffered saline (PBS), at 37°C, 5% CO_2 for trypomastigotes, and 28°C for epimastigotes. Benznidazole was used as a reference trypanocidal drug, and the absence of drug as a negative control. The viability of the parasites was estimated by determining the number of mobile forms in a Newbauer chamber (Brener, 1962). The concentration of the compound corresponding to 50% antiproliferative activity or trypanocidal activities after 72 and 24 h of incubation was expressed as IC_{50}^{epi} and IC_{50}^{try} respectively. Subsequently, the intracellular action on amastigotes was determined. Subconfluent monolayers of Vero cells were plated at 1.25×10^4 cells in RPMI supplemented with 5% FBS in each well of an eight-well chamber slide under a humidified atmosphere at 37°C, 5% CO_2, for 24 h prior to infection. Cell subconfluent monolayers were then infected with a tissue culture of trypomastigotes (12.5×10^4 parasites per well) for 24 h. After the cells had been infected, chamber slides were washed twice with cold PBS in order to remove extracellular adhered parasites, and the cells were re-incubated. Triplicate samples were treated with NO donors as described earlier. Culture media were removed 48 h post-infection and stained with Giemsa, according to the procedure previously described (Guedes *et al.*, 2007; Silva *et al.*, 2008). The number of infected cells was determined by random examination of slides and by counting a minimum of 500 cells under the microscope using high magnification (400×).

Evaluation of the trypanocidal activity in vivo *(acute model)*

Female Balb/c mice (6–8 weeks old) were infected with 1.0×10^3 BT per mouse by an i.p. injection. The animals were housed in temperature-controlled rooms (22–25°C), and received water and food *ad libitum* in the animal facilities of the Departamento de Bioquímica e Imunologia, Faculdade de Medicina de Ribeirão Preto, Universidade de São Paulo, Brazil. Test doses of the NO donors were injected orally in 100 μL of PBS as a single dose daily for 15 consecutive days. Benznidazole was used as a reference drug and was administered orally using a similar protocol. The course of infection was monitored by counting the number of mobile trypomastigotes in blood samples (5 μL) drawn from the tail veins, as described previously (Brener, 1962). The histological analyses were carried out on heart tissues of groups of five infected mice (either untreated or treated with the ruthenium complexes) 15 days after infection. The hearts were fixed in a solution of formaldehyde (10%) in PBS, embedded in paraffin, sectioned, stained with haematoxylin/eosin and examined by light microscopy.

Statistical analysis

Data are expressed as mean ± SEM. The Mann–Whitney and Kruskal–Wallis tests were used to determine the statistical significance of the inter-group comparisons. Results were considered statistically significant when $P < 0.05$.

Results

Inhibition of T. cruzi GAPDH

Recently, we showed that compounds of a series of *trans*-$[Ru(NO)(NH_3)_4L]X_n$ L = *N*-heterocyclic, H_2O, SO_3^{2-} or $P(OEt)_3$, and X = PF_6^-, BF_4^- or Cl^- (Figure 1A) have potent *in vitro* and *in vivo* anti-*T. cruzi* activity in cell culture and animal models (Silva *et al.*, 2007; 2009). The most interesting compound of the series, *trans*-$[Ru(NO)(NH_3)_4imN](BF_4)_3$, exhibited about 10-fold higher trypanocidal activity *in vivo* than gentian violet (GV) or Bz (Silva *et al.*, 2007). In the present study, we investigated the effects of these compounds on the activity of GAPDH from *T. cruzi*, a molecular target of high priority in our research group, and found that none of them inhibited this enzyme at concentrations up to 500 μM. In addition, as part of our ongoing research program aimed at discovering new anti-*T. cruzi* compounds with substantial *in vivo* activity, we synthesized a second generation of ruthenium NO donors, *cis*-$[Ru(NO)(bpy)_2imN](PF_6)_3$, *cis*-$[Ru(NO)(bpy)_21\text{-}miN](PF_6)_3$ and *cis*-$[Ru(NO)(bpy)_2SO_3]PF_6$ (Figure 1B). Interestingly, these complexes exhibited promising inhibitory effects against *T.*

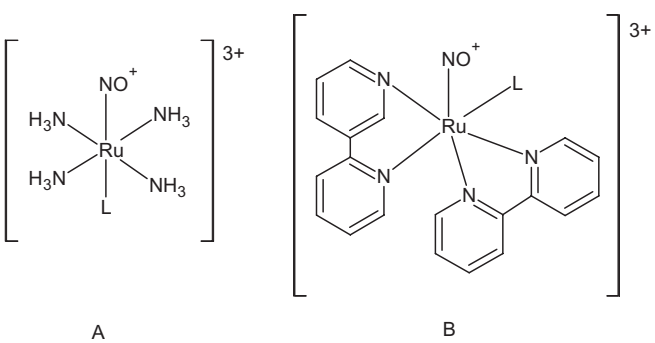

Figure 1 General structure of the rutheniumamine complexes. In the first generation, (A) L = N-heterocyclic, H_2O, SO_3^{2-} or $P(OEt)_3$, while in the second genreration, (B) L = imN, miN, and SO_3^{2-}.

Table 1 Ruthenium complexes and corresponding IC_{50} values for a series of inhibitors of *T. cruzi* GAPDH

Compound	IC_{50}^{GAPDH} *(μM)*
c-[Ru(NO)(bpy)$_2$imN](PF$_6$)$_3$	89 ± 8
c-[Ru(NO)(bpy)$_2$1-miN](PF$_6$)$_3$	97 ± 8
c-[Ru(NO)(bpy)$_2$SO$_3$]PF$_6$	153 ± 11
c-[Ru(bpy)$_2$(H$_2$O)SO$_3$]	ND[a]
c-Na[Ru(bpy)$_2$(NO$_2$)SO$_3$]	ND
c-[Ru(bpy)$_2$imN(NO$_2$)]PF$_6$	ND
c-[Ru(bpy)$_2$(H$_2$O)imN](PF$_6$)$_2$	ND
t-[Ru(NO)(bpy)$_2$SO$_3$]PF$_6$	ND
c-[Ru(NO)(NH$_3$)$_4$NO$_2$]Cl$_2$	ND
t-[Ru(NO)(NH$_3$)$_4$imN](BF$_4$)$_3$	ND

[a]ND, not determined (no inhibition observed at 500 μM).

cruzi GAPDH activity at a concentration of 200 μM, with levels of inhibition ranging from 85 to 97%. Their chemical precursors, the compounds *cis*-[Ru(bpy)$_2$(H$_2$O)SO$_3$], *cis*-Na[Ru(bpy)$_2$(NO$_2$)SO$_3$], *cis*-[Ru(bpy)$_2$imN(NO$_2$)]PF$_6$ and *cis*-[Ru(bpy)$_2$(H$_2$O)imN](PF$_6$)$_2$, which are unable to act as NO donors, exhibited no inhibitory effects on this enzyme at concentrations up to 500 μM. As can be seen in Table 1, the ruthenium compounds *cis*-[Ru(NO)(bpy)$_2$imN](PF$_6$)$_3$, *cis*-[Ru(NO)(bpy)$_2$1-miN](PF$_6$)$_3$ and *cis*-[Ru(NO)(bpy)$_2$SO$_3$]PF$_6$ exhibited substantial inhibitory activity against *T. cruzi* GAPDH, with IC_{50} values of 89, 97 and 153 μM, respectively, while IC_{50}s were not determined for other ruthenium compounds (IC_{50} >> 500 μM). The isomer *trans*-[Ru(NO)(bpy)$_2$SO$_3$]PF$_6$ and the tetraamine *cis*-[Ru(NO)(NH$_3$)$_4$NO$_2$]Cl$_2$ also did not inhibit the enzyme, suggesting that the *cis*-position of the bipyridine (bpy) groups and the nitrosyl ligands play important roles in the intermolecular interactions with the target enzyme.

Structural studies

Crystallization experiments were performed with the *T. cruzi* GAPDH enzyme and the inhibitors *cis*-[Ru(NO)(bpy)$_2$imN](PF$_6$)$_3$, *cis*-[Ru(NO)(bpy)$_2$1-miN](PF$_6$)$_3$ and *cis*-[Ru(NO)(bpy)$_2$SO$_3$]PF$_6$ to evaluate the integrity of the active cysteine site (cys166), which is a specific target for S-nitrosylation by NO donors (Bourguignon *et al.*, 1997; Hess *et al.*, 2005). Although many attempts were made, we were unable to obtain a crystal of the enzyme-inhibitor complex in order to explore the structural and mechanistic basis for enzyme inhibition. However, a crystal structure of the enzyme GAPDH that was crystallized in the presence of the complex *cis*-[Ru(NO)(bpy)$_2$SO$_3$]PF$_6$ was obtained at 1.65 Å resolution. This structure displayed a positive difference electron density at the cysteine group, compatible with S-nitrosylation (Figure 2). The details of this crystallographic structure will be published elsewhere.

As no structural data are available for an enzyme-inhibitor complex of this nature, crystallization experiments were carried out with the individual ruthenium complexes, and a crystal structure was obtained for the inhibitor *cis*-[Ru(NO)(bpy)$_2$SO$_3$]PF$_6$ (Figure 3). The structural data allowed us to evaluate the bond lengths, Ru-NO, Ru-N(bpy) and Ru-S, and the angles (bpy)N-Ru-NO and Ru-N-O. According to the

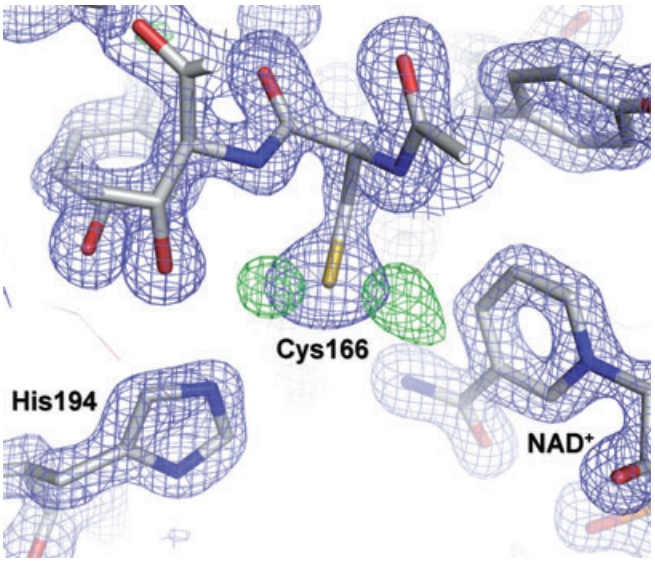

Figure 2 View of the *Trypanosoma cruzi* GAPDH NAD$^+$ binding site, showing the density maps 2Fo-Fc (s = 2.0, in blue) and Fo-Fc (s = 3.5, in green).

data collected, the Ru-N(bpy) interatomic distance for the bipyridine ligands does not change significantly, varying from 2.069 to 2.140 Å (Ru-N4 and Ru-N2 respectively). These results are in agreement with those from previous studies for similar complexes (Hamaguchi *et al.*, 2008). The Ru-S interatomic distance observed was 2.376 Å. However, the interatomic distance of the Ru-NO pair (1.746 Å) was found to be shortened relative to that of Ru-N(bpy), primarily reflecting an increase in the π character of the nitrosyl ligand. In fact, the Ru-N5-O1n angle for this complex (173.69°) is compatible with that of the fragment Ru^{II}-NO^+ (Tfouni *et al.*, 2003).

In vitro *trypanocidal activity (trypomastigote forms)*

BTs were used to infect the samples. In a standard assay, the ability of the *T. cruzi* GAPDH inhibitors to lyse BT *in vitro* was investigated. Table 2 shows the time- and concentration-dependent activities of these NO donors against BT. The nitrosyl complex *cis*-[Ru(NO)(bpy)$_2$imN](PF$_6$)$_3$ (IC_{50}^{try} = 59 μM), a GAPDH inhibitor, showed a potency similar to that of sodium nitroprusside (SNP, IC_{50}^{try} = 52 μM) and *trans*-[Ru(NO)(NH$_3$)$_4$imN](BF$_4$)$_3$ (IC_{50}^{try} = 52 μM) (Silva *et al.*, 2007), and lysed the BT cells when incubated under the same experimental conditions. Additionally, compound *cis*-[Ru(NO)(bpy)$_2$imN](PF$_6$)$_3$ exhibited about 10-fold higher trypanocidal activity than GV (IC_{50}^{try} = 536 μM) (Silva *et al.*, 2006), which is the standard drug recommended by the World Heath Organization for the treatment of *T. cruzi*-infected blood (WHO, 2005). Complexes *cis*-[Ru(NO)(bpy)$_2$1-miN](PF$_6$)$_3$ and *cis*-[Ru(NO)(bpy)$_2$SO$_3$]PF$_6$ also showed good trypanocidal activity *in vitro*, with IC_{50s}^{try} of 85 and 88 μM respectively. These compounds are over sixfold more potent than GV under standard conditions.

In vitro *anti-proliferative activity (epimastigote forms)*

In order to evaluate the biological activity of the GAPDH inhibitors, *cis*-[Ru(NO)(bpy)$_2$imN](PF$_6$)$_3$, *cis*-[Ru(NO)(bpy)$_2$1-

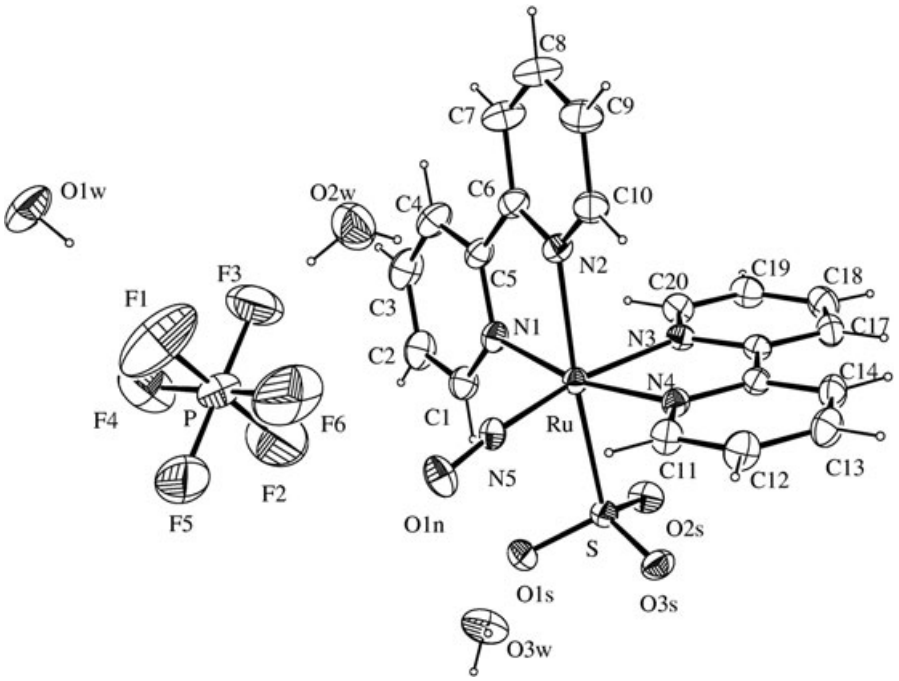

Figure 3 ORTEP view of the ruthenium complex *cis*-[Ru(NO)(bpy)$_2$SO$_3$]PF$_6$, with labelling of the atoms and the 50% probability ellipsoids.

Table 2 Trypanocidal activity of ruthenium NO donors *trans*-[Ru(NO)(NH$_3$)$_4$imN](BF$_4$)$_3$, *cis*-[Ru(NO)(bpy)$_2$imN](PF$_6$)$_3$, *cis*-[Ru(NO)(bpy)$_2$1-miN](PF$_6$)$_3$ and *cis*-[Ru(NO)(bpy)$_2$SO$_3$]PF$_6$ on trypomastigote forms in the bloodstream at different concentrations and times of incubation

Ruthenium NO donors	*Trypanocidal activity (% TA)*									
	T = 1 h			*T = 4 h*			*T = 24 h*			
	Concentration (mM)									
	0.1	*0.5*	*1*	*0.1*	*0.5*	*1*	*0.1*	*0.5*	*1*	*IC_{50}^{try} (μM)*
t-[Ru(NO)(NH$_3$)$_4$imN](BF$_4$)$_3$[a]	87 ± 6	91 ± 5	92 ± 4	68 ± 4	97 ± 3	100	97 ± 4	100	100	52
c-[Ru(NO)(bpy)$_2$imN](PF$_6$)$_3$	86 ± 7	88 ± 3	90 ± 6	78 ± 3	88 ± 6	92 ± 4	92 ± 4	97 ± 4	100	59
c-[Ru(NO)(bpy)$_2$1-miN](PF$_6$)$_3$	69 ± 8	71 ± 5	88 ± 4	67 ± 5	80 ± 4	83 ± 6	71 ± 5	79 ± 7	92 ± 4	88
c-[Ru(NO)(bpy)$_2$SO$_3$]PF$_6$	75 ± 6	79 ± 3	92 ± 4	75 ± 5	81 ± 5	87 ± 7	74 ± 8	82 ± 5	89 ± 8	85
Bz[a]	0	7 ± 6	12 ± 4	15 ± 5	21 ± 5	37 ± 7	89 ± 8	92 ± 5	100	53
SNP	56 ± 7	78 ± 3	90 ± 4	75 ± 4	89 ± 7	92 ± 4	97 ± 4	98 ± 5	100	52

Results are expressed as mean ± SEM, $n = 5–7$, $P < 0.05$. Trypanocidal activity expressed as the percentage of lysed trypomastigotes compared to the negative control. IC_{50}^{try} values correspond to 50% trypanocidal activity after 24 h of incubation.
Bz, benznidazol; SNP, sodium nitroprusside.

miN](PF$_6$)$_3$ and *cis*-[Ru(NO)(bpy)$_2$SO$_3$]PF$_6$, on replicative forms of *T. cruzi*, the effects of these compounds on *in vitro* cultures of epimastigotes were determined. Table 3 shows a summary of the results of the anti-proliferative activity of these NO donors on the exponential phase of *T. cruzi* growth expressed as the percentage of growth inhibition (% GI). As can be seen, the three complexes showed higher anti-proliferative activity ($IC_{50}^{epi} \leq 121$ μM) than both SNP ($IC_{50}^{epi} = 244$ μM) and Bz ($IC_{50}^{epi} = 3180$ μM). On the other hand, complexes *cis*-[Ru(bpy)$_2$(H$_2$O)SO$_3$], *cis*-Na[Ru(bpy)$_2$(NO$_2$)SO$_3$], *cis*-[Ru(bpy)$_2$ imN(NO$_2$)]PF$_6$ and *cis*-[Ru(bpy)$_2$(H$_2$O)imN](PF$_6$)$_2$, which do not have NO molecules in their coordination spheres, showed no substantial anti-proliferative or trypanocidal activities when incubated for up to 72 h at 1 mM (data not shown).

Effect on amastigote forms

To ensure that these compounds are able to eliminate intracellular forms of *T. cruzi*, experiments using infected Vero cells were also conducted. Figure 4 shows that compounds *cis*-[Ru(NO)(bpy)$_2$imN](PF$_6$)$_3$ and *cis*-[Ru(NO)(bpy)$_2$SO$_3$]PF$_6$ were able to eliminate amastigotes inside Vero cells, reducing the number of infected cells by 50 and 75% respectively.

In vivo *toxicity studies*

Several alternative protocols have been successfully used to replace the conventional oral LD_{50} test in order to reduce the number of animals in acute toxicity experiments (Shclede *et al.*, 2005). In the present work, we have evaluated the acute toxicity of compounds *cis*-[Ru(NO)(bpy)$_2$imN](PF$_6$)$_3$, *cis*-

Table 3 Anti-proliferative activity of the ruthenium NO donors *trans*-[Ru(NO)$(NH_3)_4$imN]$(BF_4)_3$, *cis*-[Ru(NO)$(bpy)_2$imN]$(PF_6)_3$, *cis*-[Ru(NO)$(bpy)_2$1-miN]$(PF_6)_3$ and *cis*-[Ru(NO)$(bpy)_2SO_3$]PF_6 on epimastigotes

Ruthenium NO donors	*Anti-proliferative activity (% GI)*									
	T = 1 h			*T = 4 h*			*T = 24 h*			
	Concentration (mM)									
	0.1	*0.5*	*1*	*0.1*	*0.5*	*1*	*0.1*	*0.5*	*1*	IC_{50}^{epi} *(μM)*
t-[Ru(NO)$(NH_3)_4$imN]$(BF_4)_3$[a]	16 ± 6	37 ± 4	54 ± 3	35 ± 5	39 ± 2	65 ± 4	58 ± 4	65 ± 4	78 ± 4	86
c-[Ru(NO)$(bpy)_2$imN]$(PF_6)_3$	28 ± 7	69 ± 3	76 ± 3	37 ± 2	68 ± 6	88 ± 6	49 ± 4	88 ± 8	94 ± 6	106
c-[Ru(NO)$(bpy)_2$1-miN]$(PF_6)_3$	25 ± 3	59 ± 6	66 ± 4	31 ± 2	57 ± 4	81 ± 6	45 ± 6	87 ± 3	91 ± 5	117
c-[Ru(NO)$(bpy)_2SO_3$]PF_6	27 ± 4	58 ± 9	61 ± 3	32 ± 3	55 ± 4	68 ± 4	35 ± 2	69 ± 6	84 ± 4	121
SNP[a]	19 ± 5	35 ± 2	51 ± 4	22 ± 5	56 ± 4	65 ± 3	41 ± 4	66 ± 6	74 ± 4	244
Bz	0	0	0	11 ± 3	15 ± 4	38 ± 5	15 ± 4	29 ± 4	41 ± 7	3180

Results are expressed as mean ± SEM, $n = 3–5$, $P < 0.05$. Anti-proliferative activity is expressed as the percentage of growth inhibition at the given concentration. IC_{50}^{epi} corresponds to 50% anti-proliferative activity after 72 h of incubation.
[a]Data extracted from Silva *et al.* (2008).
Bz, benznidazol; SNP, sodium nitroprusside.

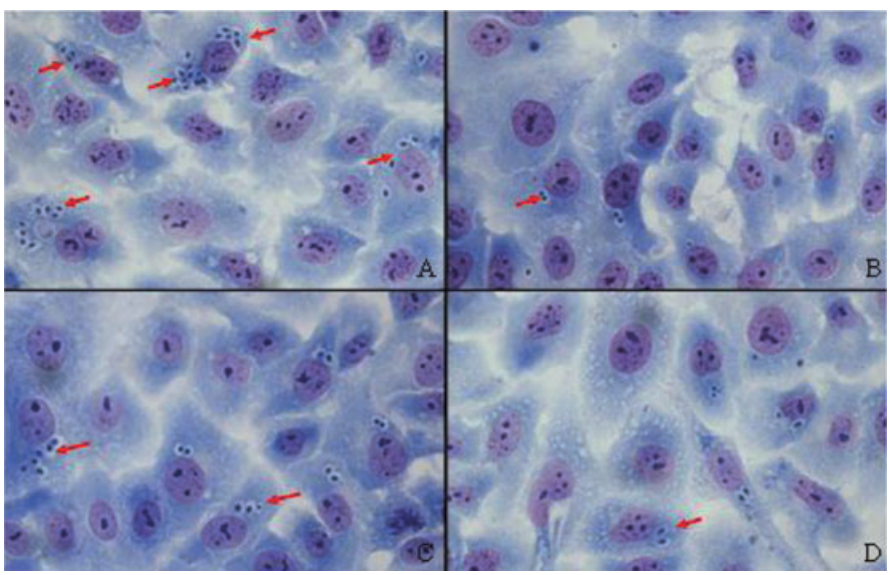

Figure 4 Vero cells infected with *T. cruzi*. The cells were cultured in cover slips for 12 h, infected with trypomastigotes of *T. cruzi* and washed with PBS. The cultures were then incubated for 48 h without (A) or in the presence of Bz (B), *cis*-[Ru(NO)$(bpy)_2$imN]$(PF_6)_3$ (C) or *cis*-[Ru(NO)$(bpy)_2SO_3$]PF_6 (D). Arrows indicate the viable amastigote forms inside the Vero cells. Note the vacuolization and absence of viable parasites in the Vero cells.

[Ru(NO)$(bpy)_2$1-miN]$(PF_6)_3$ and *cis*-[Ru(NO)$(bpy)_2SO_3$]PF_6 using the up-and-down test protocol, as previously described (Bruce, 1985). In this methodology, it is possible to evaluate the dose range and safety of the compounds for further *in vivo* assays. Non-infected Balb/c mice were treated i.p. with single doses of the compounds, ranging from 15 to 250 μmol·kg^{-1}. No acute toxic symptoms were observed in any of the animals treated for 7 days (Bruce, 1985). However, symptoms of toxicity were observed at doses as high as 500 μmol·kg^{-1}, including hyperventilation and tremors. In most cases, death occurred on the second day of treatment. Therefore, it is reasonable to assume that the true LD_{50} values for these compounds fall between 250 and 500 μmol·kg^{-1}.

In vivo *trypanocidal activity*

The trypanocidal activity of compounds *cis*-[Ru(NO)$(bpy)_2$imN]$(PF_6)_3$ and *cis*-[Ru(NO)$(bpy)_2SO_3$]PF_6 was evaluated using a murine model of acute Chagas's disease. Balb/c mice were treated, 24 h after infection, with a single daily dose of the compounds (385 nmol·kg^{-1} of body weight·day^{-1}) for 15 consecutive days (364 and 257 μg·kg^{-1}·day^{-1} for compounds *cis*-[Ru(NO)$(bpy)_2$imN]$(PF_6)_3$ and *cis*-[Ru(NO)$(bpy)_2SO_3$]PF_6 respectively). In particular, it is worth noting that the 385 nmol·kg^{-1} dose employed in these studies is approximately 650-fold lower than the highest dose to which no symptoms of toxicity were observed (250 μmol·kg^{-1}). Another group of mice was treated with

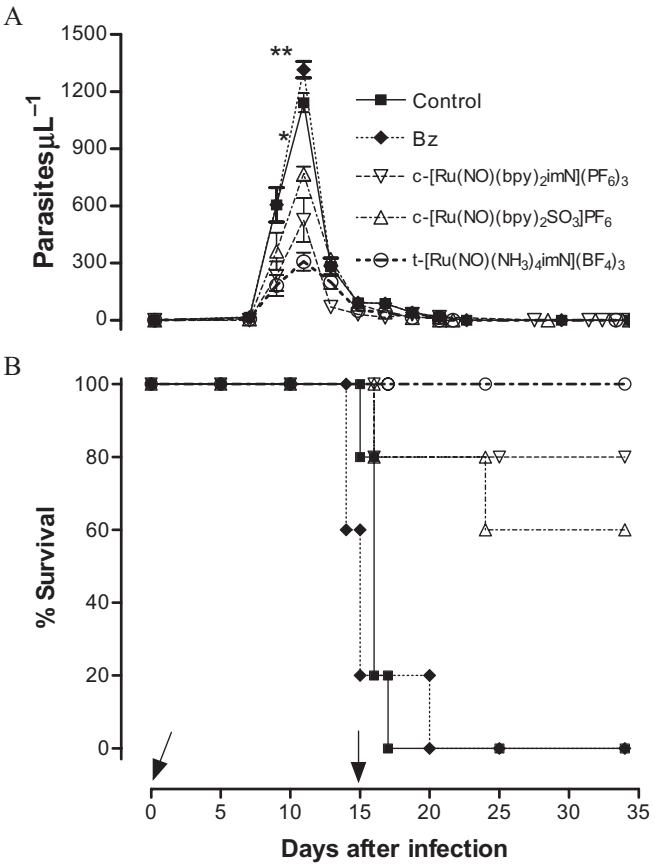

Figure 5 Parasitaemia (A) and survival rate (B) of Balb/c mice infected with *T. cruzi* and treated with *cis*-[Ru(NO)(bpy)$_2$imN](PF$_6$)$_3$, *cis*-[Ru(NO)(bpy)$_2$SO$_3$]PF$_6$ and *trans*-[Ru(NO)(NH$_3$)$_4$imN](BF$_4$)$_3$ or untreated (negative control). Mice were infected with *T. cruzi* (Y strain, 1.0×10^3 BT per mouse) and treated with each compound at a dose of 385 nmol·kg^{-1} for 15 consecutive days. Another group of infected mice was treated with Bz at the same dose (positive control). For all treatments 100 µL PBS was administered p.o. Data are representative of three independent experiments with similar results, $n = 6$.

compound *trans*-[Ru(NO)(NH$_3$)$_4$imN](BF$_4$)$_3$ under the same experimental conditions for comparative purposes. Figure 5A shows that the mice treated with compounds *cis*-[Ru(NO)(bpy)$_2$imN](PF$_6$)$_3$ and *cis*-[Ru(NO)(bpy)$_2$SO$_3$]PF$_6$ presented lower levels of parasitaemia compared with animals treated with PBS or Bz. Furthermore, 80 and 60% of the mice treated with compounds *cis*-[Ru(NO)(bpy)$_2$imN](PF$_6$)$_3$ and *cis*-[Ru(NO)(bpy)$_2$SO$_3$]PF$_6$, respectively, survived for more than 60 days, while the mice treated with a saline solution (control) or Bz at 385 nmol·kg^{-1} (100 µg·kg^{-1}) died within 20 days (Figure 5B). Taking into account the similar *T. cruzi* GAPDH inhibitory activities, as well as the comparable *in vitro* trypanocidal and anti-proliferative profiles of compounds *cis*-[Ru(NO)(bpy)$_2$imN](PF$_6$)$_3$ and *cis*-[Ru(NO)(bpy)$_2$1-miN](PF$_6$)$_3$, we decided not to evaluate the *in vivo* trypanocidal activity of compound *cis*-[Ru(NO)(bpy)$_2$1-miN](PF$_6$)$_3$ in the present study.

Cardiac inflammation in T. cruzi*-infected mice*

Histological analysis (Figure 6) of the control mice revealed the existence of several amastigote nests (intracellular forms of *T. cruzi*) in their hearts, whereas a smaller number of nests were observed in the hearts of the mice treated with the compounds *trans*-[Ru(NO)(NH$_3$)$_4$imN](BF$_4$)$_3$, *cis*-[Ru(NO)(bpy)$_2$imN](PF$_6$)$_3$ and *cis*-[Ru(NO)(bpy)$_2$SO$_3$]PF$_6$ (Figure 7B). Furthermore, the histological analysis showed that the treatment with these new NO donors decreased the occurrence of myocarditis (Figure 7A).

Discussion

There are numerous mechanisms by which mammalian cells defend themselves against free radicals (Gutierrez *et al.*, 2007). Enzymatic defence mechanisms include the use of superoxide dismutase, catalase, glutathione peroxidase and glutathione-*S*-transferases. Non-enzymatic mechanisms involve reductive compounds such as α-tocopherol, ascorbate, β-carotene and reduced glutathione (GSH). In contrast, no catalase or glutathione peroxidase activity has been detected in *T. cruzi*, and the superoxide dismutase activity is very low (Turrens, 2004). In addition, there is no evidence for the existence of α-tocopherol or β-carotene in the parasite. Thus, reduced glutathione and the trypanothione/trypanothione reductase system represent the principal mechanism for the parasite's defence against oxidative stress (Opperdoes, 1985). In addition, the vital dependence on glycolysis as a source of energy for the infective trypomastigote forms of trypanosomatids makes this metabolic pathway particularly attractive for drug design (Opperdoes, 1985; Verline *et al.*, 2001).

The glycolytic enzyme GAPDH catalyses the reversible oxidative phosphorylation of glyceraldehyde-3-phosphate (G-3-P) to 1,3-bisphosphoglycerate (1,3-DPG) in the presence of NAD$^+$ and inorganic phosphate. The tetrameric enzyme GAPDH has four subunits composed of two domains (an N-terminal or NAD$^+$ binding domain, and a C-terminal or catalytic domain). The N-terminal domain contains the loop formed by specific residues found only in the GAPDHs of the Trypanosomatidae family, whereas the catalytic domain includes the amino acid residues cysteine (Cys166) and histidine (His194), which are essential for catalytic activity (Souza *et al.*, 1998). The crucial Cys166 residue is located within the central region of the *T. cruzi* GAPDH active site and has been described as a nucleophilic agent that reacts with G-3-P to form a thiohemiacetal intermediate, followed by the formation of a thioester. Therefore, it is a potential target for selective reaction with nitrosyl complexes, thus impeding the formation of the covalent intermediate Cys166-G-3-P and, consequently, the subsequent proton transfer to the NAD cofactor, which occurs during the dehydrogenation step (Souza *et al.*, 1998).

In the present work, we have investigated both GAPDH and thiol metabolism in *T. cruzi* as possible targets for the *in vitro* and *in vivo* trypanocidal activity of *cis*-[Ru(NO)(bpy)$_2$imN](PF$_6$)$_3$ and *cis*-[Ru(NO)(bpy)$_2$SO$_3$]PF$_6$. The crystal structure of the enzyme revealed a positive difference in the density at Cys166, which suggests an S-nitrosylation mechanism at the active thiol site (Figure 2). These molecular events would be directly involved in the observed inhibition of GAPDH, because the sulphur atom of the modified Cys166

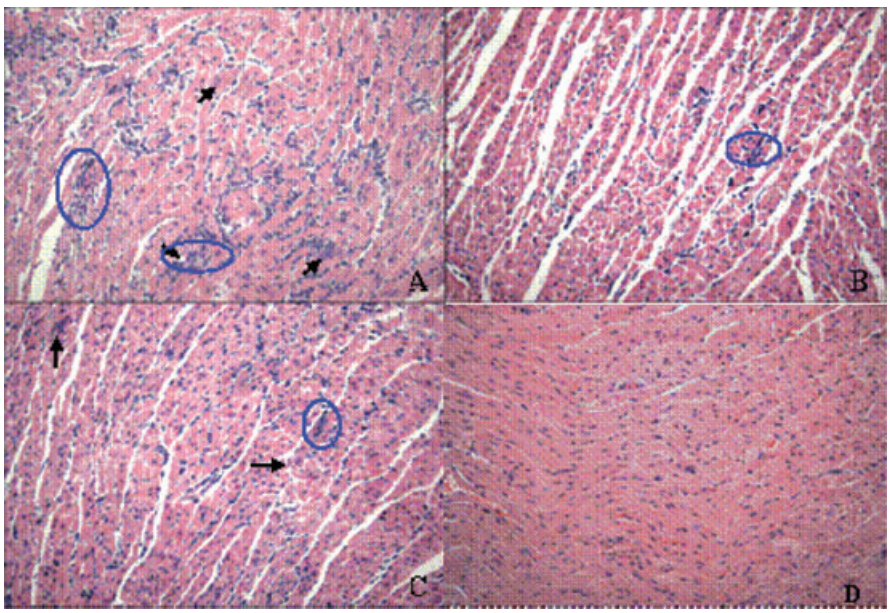

Figure 6 Histological patterns of heart sections of mice infected with *Trypanosoma cruzi* 1.0×10^3 BT per mouse and treated with (A) PBS, (B) *cis*-$[Ru(NO)(bpy)_2imN](PF_6)_3$, (C) *cis*-$[Ru(NO)(bpy)_2SO_3]PF_6$ and (D) *trans*-$[Ru(NO)(NH_3)_4imN](BF_4)_3$ for 15 consecutive days. After the 15-day test period, the mice were killed and their hearts processed using a haematoxylin and eosin stain. Note that the intensity of the inflammatory process with mononuclear cell infiltrates and necrosis in (A), but not in (B), (C), or (D). Black arrows indicate the nests of amastigotes, while circles indicate inflammatory cells. Photomicrographs are representative of three independent experiments with similar results. Final magnification: 200X.

is no longer available as a nucleophile to form the thiohemiacetal intermediate. It could also explain why the nitrosyl complexes *cis*-$[Ru(bpy)_2(H_2O)SO_3]$, *cis*-$Na[Ru(bpy)_2(NO_2)SO_3]$, *cis*-$[Ru(bpy)_2imN(NO_2)]PF_6$ and *cis*-$[Ru(bpy)_2(H_2O)imN](PF_6)_2$, which do not act as NO donors, showed no inhibition of *T. cruzi* GAPDH activity at 500 μM. There is significant evidence suggesting that NO plays an important role in a variety of physiological, pathological and pharmacological processes (Pacher *et al.*, 2007), and GAPDH has been implicated in the intracellular events mediated by NO (Mohr *et al.*, 1996). It has been shown that NO-induced covalent modifications of the active cysteine site is dependent on NAD^+ and occurs via the transient formation of an *S*-nitrosothiol intermediate, which inactivates the enzyme (Mohr *et al.*, 1994; Bourguignon *et al.*, 1997). It has also been found that peroxynitrite (ONO_2^-), a product of the reaction between NO and superoxide ions ($O2^{\bullet-}$) or nitroxyl (HNO/NO^-) and molecular oxygen (Pacher *et al.*, 2007), can mediate the inactivation of GAPDH via the NAD(H)-dependent covalent modification (Souza and Radi, 1998). Furthermore, inhibition of GAPDH by HNO has recently been discussed (Lopez *et al.*, 2007), and HNO can also be a product of the reactions of nitrosyl complexes with R-SH groups (Roncaroli and Olabe, 2005).

It has previously been shown that the complexes *cis*-$[Ru(NO)(bpy)_2imN](PF_6)_3$ and *cis*-$[Ru(NO)(bpy)_2SO_3]PF_6$ release NO through electrochemical, photochemical and chemical processes (Da Silva *et al.*, 2006). The reactions of these complexes with sulphydril compounds, such as glutathione and cysteine, could lead to the formation of an aqua species and free nitric oxide according to the following mechanism:

$$[(bpy)_2LRuNO]^n \underset{-RS^-}{\overset{RS^-}{\rightleftharpoons}} [(bpy)_2LRuN(O)SR]^{n-1} \underset{-RS^-}{\overset{RS^-}{\rightleftharpoons}} [(bpy)_2LRuN(O)(SR)_2]^{n-2} \rightarrow [(bpy)_2LRu(H_2O)]^{n-1} + NO^0 + RSSR$$

The rate constant of this reaction is pH dependent and increases with increasing pH, due to the acid–base equilibrium of the thiol group of the cysteine residue. The formation of the two intermediates is very fast (on the stopped flow scale) compared with the rate of NO production (in the final step). The process of labilization of the nitrosyl ligand, starting from the reaction of the compounds with sulphydrils, was spectrophotometrically monitored as a function of reaction time (Figure 8). Moreover, the signal recorded by the NO sensor was observed when the reaction with glutathione or cysteine was initiated, which indicated the presence of free NO (results not shown).

In summary, the data obtained strongly suggest that the *cis*-$[Ru(NO)(bpy)_2L](PF_6)_n$ compounds are effective against *T. cruzi in vivo*, and one of their mechanisms of action is via S-nitrosylation of the active Cys166 site of the enzyme GAPDH according to the following reaction:

$$c\text{-}[Ru^{II}NO^+]^n + Cys166 \leftrightarrow c\text{-}[Ru^{II}N(O)S_{Cys166}]^{n-1} \rightarrow c\text{-}[Ru^{II}OH_2]^{n-1} + NOS_{Cys166}$$

In addition, because these complexes react easily with glutathione and potentially with trypanothione, it is reasonable to suggest that they can also act through the trypanothione/trypanothione reductase system. Further studies are needed to

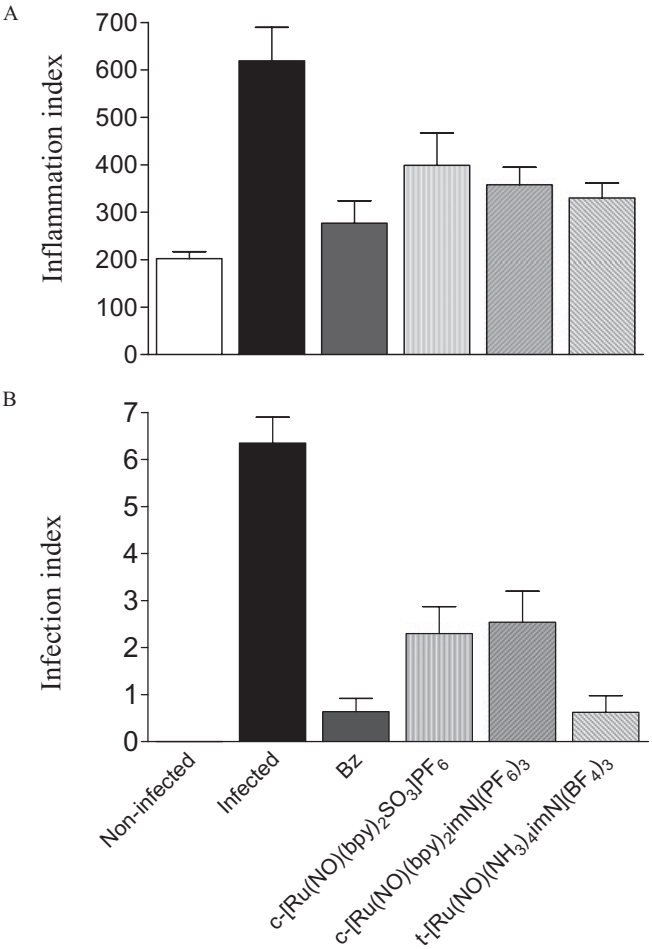

Figure 7 (A) Inflammation index and (B) infection index quantified from the histological analysis. The mice were infected with *T. cruzi* 1.0×10^3 BT per mouse and treated with PBS (infected), *cis*-$[Ru(NO)(bpy)_2imN](PF_6)_3$, *cis*-$[Ru(NO)(bpy)_2SO_3]PF_6$ and *trans*-$[Ru(NO)(NH_3)_4imN](BF_4)_3$ for 15 consecutive days. After the 15-day test period, the mice were killed and their hearts processed with a haematoxylin and eosin stain. After this, the number of cellular nucleous was quantified in 50 μm^{-2} of heart tissue for inflammation index, and number of amastigote nests quantified in 245.76 μm^{-2} of heart tissue using the program imagingJ. For comparison, a group of non-infected mice were killed and their hearts processed similarly. Data represent mean ± SEM, $n = 3$.

elucidate this mechanism of action, as well as that of the enzymatic inhibition (e.g. cruzain).

Acknowledgements

We gratefully acknowledge the financial support from Fundação de Amparo à Pesquisa do Estado de São Paulo, Conselho Nacional de Desenvolvimento Científico e Tecnológico (CNPq), Coordenação de Aperfeiçoamento de Pessoal de Nível Superior and the Millennium Institute for Vaccine Development and Technology (MIVDT/CNPq). The authors thank Dr Rafael V.C. Guido, Gustavo Mercaldi and Prof. Richard C. Garratt for their assistance in the discussion of some of the experiments.

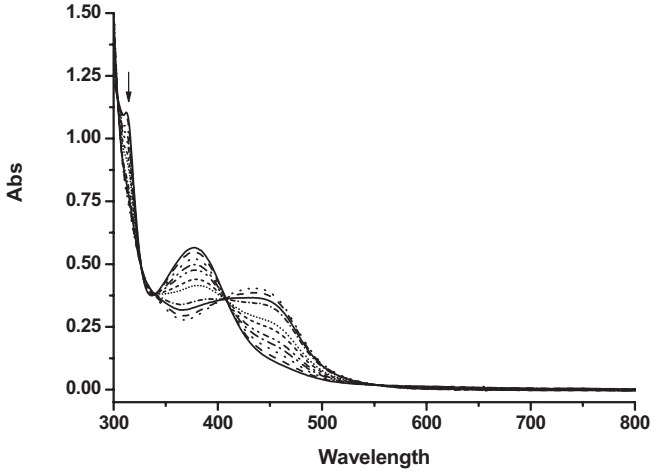

Figure 8 Electronic spectra for the reaction of complex *cis*-$[Ru(NO)(bpy)_2SO_3]PF_6$ with glutathione. Temperature = 25°C, μ = 1 mM and pH = 7.2.

Conflict of interest

None.

References

Blessing RH (1995). An empirical correction for absorption anisotropy. *Acta Crystallogr A* **A51**: 33–38.

Borges SSS, Davanzo CU, Castellano EE, Z-Zchpector J, Silva SC, Franco DW (1998). Ruthenium nitrosyl complexes with N-heterocyclic ligands. *Inorg Chem* **37**: 2670–2677.

Bourguignon SC, Alves CR, Giovanni-De-Simone S (1997). Detrimental effect of nitric oxide on *Trypanosoma cruzi* and *Leishmania major* like cells. *Acta Trop* **66**: 109–118.

Brener Z (1962). Therapeutic activity and criterion of cure on mice experimentally infected with *Trypanosoma cruzi*. *Rev Inst Med Trop Sao Paulo* **4**: 389–396.

Bruce RD (1985). An up-and-down procedure for acute toxicity testing. *Fundam Appl Toxicol* **5**: 151–157.

Castro JA, Meca MM, Bartel LC (2006). Toxic side effect of drugs used to treat Chagas's disease (American trypanosomiasis). *Hum Exp Toxicol* **25**: 471–479.

Da Silva FON, Araújo SXB, Holanda AKM, Meyer E, Sales FAM, Diógenes ICN *et al*. (2006). Synthesis, characterization and NO release study of *cis*- and *trans*-$[Ru(Bpy)2(SO_3)NO]^+$ complexes. *Eur J Inorg Chem* **2006**: 2020–2026.

Engels D, Savioli L (2006). Reconsidering the underestimated burden caused by neglected tropical diseases. *Trends Parasitol* **22**: 363–366.

Enraf-Nonius (1997). *COLLECT*. Nonius BV: Delft, The Netherlands.

Farrugia LJJ (1997). *ORTEP3* for Windows. *J Appl Crystallogr* **30**: 565.

Farrugia LJJ (1999). WinGX. WinGX suite for small-molecule single-crystal crystallogrraphy. *J Appl Crystallogr* **32**: 837–838.

Guedes PMM, Veloso VM, Caliari MV, Carneiro CM, Souza SM, de Lana M *et al*. (2007). *Trypanosoma cruzi* high infectivity *in vitro* is related to cardiac lesions during long-term infection in Beagle dogs. *Mem Inst Oswaldo Cruz* **102**: 141–147.

Guido RVC, Oliva G, Montanari CA, Andricopulo AD (2008). Structural basis for selective inhibition of trypanosomatid glyceraldehyde-3-phosphate dehydrogenase: molecular docking and 3D QSAR studies. *J Chem Inf Model* **48**: 918–929.

Gutierrez FRS, Mariano FS, Miranda-Santos IKF, Silva JS (2007). Effector mechanisms of macrophages infected with *Trypanosoma cruzi*. In: Denkers EY, Gazzinelli RT (eds). *Protozoans in Macrophages*, 1st edn. Medical Intelligence Unit, Landes Bioscience: Austin, TX, pp. 207–220.

Hamaguchi T, Inoue Y, Ujimoto K, Ando I (2008). Synthesis, crystal structure and electrochemistry of a ruthenium complex coordinated with an ambidentate 2-mercaptopyridinato *N*-oxide ligand. *Polyhedron* **27**: 2031–2034.

Hess DT, Matsumoto A, Kim SO, Marshall HE, Stamler JS (2005). Protein S-nitrosylation: purview and parameters. *Nat Rev Mol Cell Biol* **6**: 150–166.

Lopez BE, Wink DA, Fukuto JM (2007). The inhibition of glyceraldehyde-3-phosphate dehydrogenase by nitroxyl (HNO). *Arch Biochem Biophys* **465**: 430–436.

Maya JD, Cassels BK, Iturriaga-Vásquez P, Ferreira J, Faúdez M, Galanti N *et al*. (2007). Mode of action of natural and synthetic drugs against *Trypanosoma cruzi* and their interaction with mammalian host. *Comp Biochem Physiol A Mol Integr Physiol* **146**: 601–620.

Mohr S, Stamler JS, Brüne B (1994). Mechanism of covalent modification of glyceraldehyde-3-phosphate dehydrogenase at its active site thiol by nitric oxide, peroxynitrite and related nitrosating agents. *FEBS Lett* **348**: 223–227.

Mohr S, Stamler JS, Brüne B (1996). Posttranslational modification of glyceraldehyde-3-phosphate dehydrogenase by S-nitrosylation and subsequent NADH attachment. *J Biol Chem* **271**: 4209–4214.

Opperdoes FR (1985). Biochemical peculiarities of *Trypanosoma african* and *south american*. *Br Med Bull* **41**: 130–136.

Otwinowski Z, Minor W, Denzo HKL (1997). Scalepack. In: Carter CW Jr, Sweet RM (eds). *Methods in Enzymology*, Vol. 276. Academic Press: New York, pp. 307–326.

Pacher P, Beckman JS, Liaudet L (2007). Nitric oxide and peroxynitrite in health and disease. *Physiol Rev* **87**: 315–424.

Pereira JM, Severino RP, Vieira PC, Fernandes JB, da Silva MFGF, Zottis A *et al*. (2008). Anacardic acid derivatives as inhibitors of glyceraldehyde-3-phosphate dehydrogenase from *Trypanosoma cruzi*. *Bioorg Med Chem* **16**: 8889–8895.

Reddy M, Gill SS, Kalkar SR, Wu W, Anderson PJ, Rochon PA (2007). Oral drug therapy for multiple neglected tropical diseases: a systematic review. *JAMA* **298**: 1911–1924.

Roncaroli F, Olabe JA (2005). The reactions of nitrosyl complexes with cysteine. *Inorg Chem* **44**: 4719–4727.

Sachs JD (2007). The neglected tropical diseases. *Sci Am* **296**: 33A.

Shclede E, Genschow E, Spielmann H, Stropp G, Kayser D (2005). Oral acute toxic class: a successful alternative to the oral LD_{50} test. *Regul Toxicol Pharmacol* **42**: 15–23.

Sheldrick GM (1997). *SHELXS-97*. Program for crystal structure resolution. Univ. of Göttingen: Göttingen, Germany.

Silva LHP, Nussenzweig V (1953). Sobre uma cepa altamente virulenta para o camundongo branco. *Folia Clin Biol (Sao Paulo)* **20**: 191–208.

Silva JS, Machado FS, Martins GA (2003). The role of nitric oxide in the pathogenesis of Chagas' disease. *Front Biosci* **1**: s314–s325.

Silva RSF, Costa EM, Trindade ULT, Teixeira DV, Pinto MCFR, Santos GL *et al*. (2006). Synthesis of naphthofuranquinones with activity against *Trypanosoma cruzi*. *Eur J Med Chem* **41**: 526–530.

Silva JJN, Osakabe AL, Pavanelli WR, Silva JS, Franco DW (2007). *In vitro* and *in vivo* antiproliferative and trypanocidal activities of ruthenium NO donors. *Br J Pharmacol* **152**: 112–121.

Silva JJN, Pavanelli WR, Gutierrez FRS, Lima FCA, da Silva ABF, Silva JS *et al*. (2008). Complexation of the anti-*Trypanosoma cruzi* drug benznidazole improves solubility and efficacy. *J Med Chem* **51**: 4104–4114.

Silva JJN, Pavanelli WR, Pereira JCM, Silva JS, Franco DW (2009). Experimental chemotherapy against *Trypanosoma cruzi* infection using ruthenium nitric oxide donors. *Antimicrob Agents Chemother* **53**: 50–58.

Souza JM, Radi R (1998). Glyceraldehyde-3-phosphate dehydrogenase inactivation by peroxynitrite. *Arch Biochem Biophys* **360**: 187–194.

Souza DHF, Garratt RC, Araújo APU, Guimarães BG, Jesus WDP, Michels PAM *et al*. (1998). *Trypanosoma cruzi* glycosomal glyceraldehyde-3-phosphate dehydrogenase: structure, catalytic mechanism and targeted inhibitor design. *FEBS Lett* **424**: 131–135.

Tfouni E, Krieger M, McGarvey B, Franco DW (2003). Structure, chemical and photochemical reactivity and biological activity of some ruthenium nitrosyl complexes. *Coord Chem Rev* **236**: 57–69.

Turrens JF (2004). Oxidative stress and antioxidant defenses: a target for the treatment of diseases caused by parasitic protozoa. *Mol Aspects Med* **25**: 211–220.

Verline CLMJ, Hannaert V, Blonski C, Willson M, Périé JJ, Fathergill-Gilmore LA *et al*. (2001). Glycolysis as target for the design of new anti-trypanosome drugs. *Drug Resist Updat* **4**: 1–14.

World Health Organization (WHO) (2005). Tropical disease research: progress 2003–2004 seventeenth programme report of the UNICEF/UNDP/World Bank/WHO. In: Chan M, Heymann D, Ridley R (eds). *Special Programme for Research & Training in Tropical Diseases (TDR)*. World Health Organization: Geneva, pp. 31–33.